ELSEVIER

Journal of Organometallic Chemistry 530 (1997) 105–115

Journal of Organometallic Chemistry

# Structure and bonding in a series of cyano complexes: $RuCp(PPh_3)_2CN$, $[RuCp(PPh_3)_2(CNH)]CF_3SO_3$, and H-bridged $[Ru_2(Cp)_2(PPh_3)_4CNHNC]CF_3SO_3$

V.N. Sapunov [a,1], K. Mereiter [b], R. Schmid [a], K. Kirchner [a,*]

[a] *Institute of Inorganic Chemistry, Technical University of Vienna, Getreidemarkt 9, A-1060, Vienna, Austria*

[b] *Institute of Mineralogy, Crystallography and Structural Chemistry, Technical University of Vienna, Getreidemarkt 9, A-1060, Vienna, Austria*

Received 2 May 1996; revised 10 June 1996

**Abstract**

The three title cyanoruthenium complexes have been characterized by means of X-ray diffraction analysis, IR and NMR solution spectroscopies, as well as extended Hückel molecular orbital calculations examining the properties of the cyanide fragment changing with complexation and with the co-ligands Cp and $PPh_3$. Explanations are given for crystallographic results of the C–N bond shortening upon complexation, the supershort (2.573 Å) bond length of N(H) · · · N in the bridged complex, as well as the Ru–C–N and C–N–H–N–C bendings. Although the crystallographically found asymmetry of coordinated Cp is not significant, the MO calculations suggest a distorted endocyclic bond-length pattern indicative of the relative importance of $\sigma$ and $\pi$ bonding in the metalcyclopentadienyl interactions.

*Keywords:* Ruthenium; Cyanide; Cyclopentadienyl; Extended Hückel calculations; Hydrogen bonding; Hydrogen isocyanide

## 1. Introduction

It is now well-established that the cyanide ion, combined with a suitable metal complex fragment containing electron-rich co-ligands, is a versatile reagent on which an extensive chemistry can be based [1]. For example, the cyano ligand in complexes of the type $MCpL_2CN$ (M = Fe, Ru; Cp = $\eta^5$-$C_5H_5$; L = tertiary phosphines) is readily converted with strong electrophiles such as $R_3O^+BF_4^-$ (R = Me, Et), $H^+$ or weak electrophiles such as alkyl halides (RX) to form the corresponding cationic isocyanide complexes [2,3] The metal-stabilized, $\eta^1$-coordinated 'isoprussic acid', in turn, is a strong Lewis acid capable of forming –CN(H) · · · NC– bridges with 'super-short' hydrogen bonds [1]. While isocyanide complexes are ubiquitous in transition metal chemistry, few hydrogen isocyanide complexes have been isolated and characterized [1]. Evidence of the presence of CNH ligands, however, stems mainly from chemical plausibility, IR and NMR spectroscopy, whereas only few X-ray structural investigations have been reported [1].

Here we undertake comparative studies of two known complexes $RuCp(PPh_3)_2CN$, $[RuCp(PPh_3)_2(CNH)]CF_3SO_3$ and the new H-bridged complex $[Ru_2Cp_2(PPh_3)_4(\mu\text{-}CN(H)NC)]CF_3SO_3$. In addition to spectroscopic and X-ray investigations, we also include extended Hückel (EH) molecular orbital calculations in order to more fully characterize the structure and bonding of the complexes overall, and in particular of the bridging ligand in the dimer. Whereas ab inito calculation on $(HCN)_n$ clusters suggest a linear construction [4], X-ray crystallography of hydrogen-bonded adducts of CNH point to CN(H) · · · NC bonds that deviate up to 20° from linearity [1].

## 2. Experimental section

### 2.1. General methods

All manipulations were performed in air. All chemicals were standard reagent grade and used without

* Corresponding author.

[1] On leave of absence from D. Mendeleyev University of Chemical Technology of Russia, Miusskaja 9, 125047 Moscow, Russia.


*PII* S0022-328X(96)06603-X

further purification. The solvents were purified according to standard procedures [5]. The deuterated solvents were purchased from Aldrich and dried over 4 Å molecular sieves. IR spectra were obtained on a Mattson RSI FTIR spectrometer. $^{1}H$ and $^{13}C\{^{1}H\}$ NMR spectra were recorded on a Bruker AC 250 spectrometer and were referenced to $SiMe_4$. Microanalyses were conducted by Microanalytical Laboratories, University of Vienna, Austria.

### 2.1.1. Synthesis of $RuCp(PPh_3)_2CN$ (1)

$RuCp(PPh_3)_2CN$ (**1**) was prepared as described in the literature [2,3]. $^{1}H$ NMR (250.13 MHz, $\delta$, $CD_2Cl_2$, 20 °C): 7.39–7.13 (m, 30H, Ph), 4.39 (s, 5H, Cp). $^{13}C\{^{1}H\}$ NMR (62.86 MHz, $\delta$, $CD_2Cl_2$, 20 °C): 142.0 (t, $^{2}J(CP) = 19.9$ Hz, CN), 138.2, 133.6, 129.3, 127.8, 85.3 (t, $^{2}J(CP) = 1.9$ Hz, Cp). IR $\nu/cm^{-1}$ (poly(chlorotrifluoroethylene)) 2070 (s, CN).

### 2.1.2. Synthesis of $[RuCp(PPh_3)_2(CNH)]CF_3SO_3$ (2)

A solution of **1** (432 mg, 0.603 mmol) in $CH_2Cl_2$ (5 ml) was treated with 1.5 equivalents of $CF_3SO_3H$, whereupon an immediate color change from yellow to green was observed. The reaction is quantitative as followed by $^{1}H$ NMR spectroscopy. On addition of anhydrous diethyl ether, **2** precipitated and was collected on a glass-frit, washed with anhydrous diethyl ether and dried under vacuum. Yield: 467 mg (89%). Anal. Found: C, 59.11; H, 3.90; N, 1.58; P, 7.36; S, 3.59. $C_{43}H_{36}F_3NO_3P_2RuS$. Calc.: C, 59.58; H, 4.19; N, 1.62; P, 7.15; S, 3.70%. $^{1}H$ NMR (250.13 MHz, $\delta$, $CD_2Cl_2$, 20 °C): 7.38–7.11 (m, 30H, Ph), 4.62 (s, 5H, Cp). $^{13}C\{^{1}H\}$ NMR (62.86 MHz, $\delta$, $CD_2Cl_2$, 20 °C): 136.5, 133.3, 130.3, 128.5, 87.6 (t, $^{2}J(CP) = 1.7$ Hz, Cp). IR $\nu/cm^{-1}$ (poly(chlorotrifluoroethylene)): 2016 (w, CN).

### 2.1.3. Synthesis of $[Ru_2Cp_2(PPh_3)_4(\mu\text{-}CNH\text{-}NC)]CF_3SO_3 \cdot 1.5CH_2Cl_2$ ($3 \cdot 1.5CH_2Cl_2$)

Equimolar solutions of **1** and **2** in $CH_2Cl_2$ were stirred for 2 h at 40 °C. The mixture was placed in a closed vial with diethyl ether for 1 day, whereupon green-yellow crystals of **3** in the form of the solvate $3 \cdot 1.5CH_2Cl_2$ were formed. Yield: greater than 95%. Anal. Found: C, 61.82; H, 4.39; N, 1.69; P, 7.52; S, 1.99. $C_{86.5}H_{74}Cl_3F_3N_2O_3P_4Ru_2S$. Calc.: C, 60.72; H,

Table 1
Crystallographic data and data collection for $1 \cdot CH_2Cl_2$, **2**, and $3 \cdot 1.5CH_2Cl_2$ [a]

| | $1 \cdot CH_2Cl_2$ | **2** | $3\,1.5CH_2Cl_2$ |
|---|---|---|---|
| Formula | $C_{43}H_{37}Cl_2NP_2Ru$ | $C_{43}H_{36}F_3NO_3P_2RuS$ | $C_{86.5}H_{74}Cl_3F_3N_2O_3P_4Ru_2S$ |
| Fw | 801.65 | 866.80 | 1710.91 |
| Crystal system | triclinic | monoclinic | triclinic |
| Crystal size ($mm^3$) | $0.42 \times 0.44 \times 0.48$ | $0.18 \times 0.33 \times 0.72$ | $0.20 \times 0.30 \times 0.40$ |
| Space group | $P\bar{1}$ (No. 2) | $P2_1/n$ (No. 14) | $P\bar{1}$ (No. 2) |
| $a$ (Å) | 9.890(2) | 12.990(3) | 13.884(2) |
| $b$ (Å) | 14.147(3) | 16.983(4) | 15.343(3) |
| $c$ (Å) | 14.431(3) | 17.720(4) | 20.580(3) |
| $\alpha$ (deg) | 99.55(1) | | 76.37(1) |
| $\beta$ (deg) | 106.16(1) | 99.07(1) | 72.62(1) |
| $\gamma$ (deg) | 99.80(1) | | 80.00 (1) |
| $V$ (Å$^3$) | 1862(1) | 3860(2) | 4041(1) |
| $Z$ | 2 | 4 | 2 |
| $\rho_{calc}$ ($g\,cm^{-3}$) | 1.430 | 1.491 | 1.406 |
| $T$ (K) | 295 | 293 | 294 |
| $\mu$(Mo K$\alpha$) ($mm^{-1}$) | 0.682 | 0.600 | 0.634 |
| Absorption corr. | none | analytical | none |
| Transmission factor min/max | | 0.85/0.92 | |
| $\theta_{max}$ (deg) | 25 | 25 | 25 |
| Index ranges | $-11 \le h \le 11$ | $-15 \le h \le 15$ | $-15 \le h \le 16$ |
| | $-16 \le k \le 16$ | $0 \le k \le 20$ | $-17 \le k \le 18$ |
| | $0 \le l \le 17$ | $0 \le l \le 21$ | $0 \le l \le 24$ |
| No. of reflections measured | 6549 | 7494 | 14271 |
| No. of unique reflections | 6549 | 6784 | 14252 |
| No. of reflections $F > 4\sigma(F)$ | 6016 | 6770 | 14245 |
| No. of parameters | 443 | 495 | 928 |
| $R(F)$ ($F > 4\sigma(F)$) | 0.0238 | 0.0433 | 0.0516 |
| $R(F)$ (all data) | 0.0274 | 0.0637 | 0.0840 |
| $wR(F^2)$ (all data) | 0.0602 | 0.1154 | 0.1395 |
| Diff. Fourier peaks min/max (e Å$^{-3}$) | −0.46/0.47 | −0.45/0.68 | −0.93/0.76 |

[a] Philips PW 1100 four-circle diffractometer, $\theta$–$2\theta$ scans.

4.36; N, 1.64; P, 7.24; S, 1.87%. $^1$H NMR (250.13 MHz, $\delta$, $CD_2Cl_2$, 20 °C): 7.31–7.12 (m, 60H, Ph), 4.52 (s, 10H, Cp). $^{13}C\{^1H\}$ NMR (62.86 MHz, $\delta$, $CD_2Cl_2$, 20 °C): 149.8 (t, $^2J(CP) = 19.7$ Hz, CN), 137.1, 133.7, 130.0, 128.3, 86.7 (t, $^2J(CP) = 1.8$ Hz, Cp). IR $\nu/cm^{-1}$ (poly(chlorotrifluoroethylene)) 2084 (s, CN).

Table 2
Atomic coordinates and equivalent isotropic displacement parameters ($Å^2 \times 10^3$) for $[RuCp(PPh_3)_2CN]\cdot CH_2Cl_2$ ($1\cdot CH_2Cl_2$)

| | x | y | z | $U_{eq}$ |
|---|---|---|---|---|
| Ru | 0.59919(2) | 0.23782(1) | 0.19748(1) | 28(1) |
| C(1) | 0.4983(2) | 0.1380(2) | 0.0470(2) | 42(1) |
| C(2) | 0.4703(2) | 0.2331(2) | 0.0426(2) | 44(1) |
| C(3) | 0.3864(2) | 0.2536(2) | 0.1040(2) | 48(1) |
| C(4) | 0.3616(2) | 0.1725(2) | 0.1478(2) | 47(1) |
| C(5) | 0.4310(2) | 0.1018(2) | 0.1122(2) | 45(1) |
| P(1) | 0.80542(5) | 0.31637(3) | 0.17238(3) | 30(1) |
| C(6) | 0.8315(2) | 0.2442(1) | 0.0633(2) | 38(1) |
| C(7) | 0.8819(3) | 0.1588(2) | 0.0695(2) | 55(1) |
| C(8) | 0.8841(3) | 0.0975(2) | −0.0162(3) | 80(1) |
| C(9) | 0.8380(3) | 0.1206(2) | −0.1070(2) | 79(1) |
| C(10) | 0.7869(3) | 0.2028(2) | −0.1135(2) | 69(1) |
| C(11) | 0.7837(3) | 0.2646(2) | −0.0298(2) | 49(1) |
| C(12) | 0.7986(2) | 0.4356(1) | 0.1373(1) | 35(1) |
| C(13) | 0.9176(2) | 0.4868(2) | 0.1186(2) | 47(1) |
| C(14) | 0.9160(3) | 0.5762(2) | 0.0915(2) | 57(1) |
| C(15) | 0.7969(3) | 0.6160(2) | 0.0840(2) | 58(1) |
| C(16) | 0.6793(3) | 0.5670(2) | 0.1030(2) | 57(1) |
| C(17) | 0.6799(2) | 0.4763(2) | 0.1296(2) | 44(1) |
| C(18) | 0.9847(2) | 0.3549(1) | 0.2657(1) | 35(1) |
| C(19) | 0.9982(2) | 0.4230(2) | 0.3507(2) | 44(1) |
| C(20) | 1.1306(2) | 0.4619(2) | 0.4221(2) | 53(1) |
| C(21) | 1.2519(2) | 0.4323(2) | 0.4099(2) | 58(1) |
| C(22) | 1.2404(3) | 0.3661(2) | 0.3262(2) | 64(1) |
| C(23) | 1.1083(2) | 0.3271(2) | 0.2534(2) | 51(1) |
| P(2) | 0.68626(5) | 0.15908(4) | 0.32261(4) | 33(1) |
| C(24) | 0.7625(2) | 0.0521(1) | 0.2946(2) | 39(1) |
| C(25) | 0.7478(2) | 0.0092(2) | 0.1979(2) | 48(1) |
| C(26) | 0.8001(3) | −0.0743(2) | 0.1757(2) | 63(1) |
| C(27) | 0.8659(3) | −0.1157(2) | 0.2505(2) | 69(1) |
| C(28) | 0.8809(3) | −0.0747(2) | 0.3468(2) | 65(1) |
| C(29) | 0.8301(3) | 0.0085(2) | 0.3689(2) | 55(1) |
| C(30) | 0.8192(2) | 0.2238(1) | 0.4432(1) | 38(1) |
| C(31) | 0.7798(3) | 0.2555(2) | 0.5264(2) | 56(1) |
| C(32) | 0.8847(4) | 0.3023(2) | 0.6161(2) | 70(1) |
| C(33) | 1.0277(3) | 0.3191(2) | 0.6243(2) | 66(1) |
| C(34) | 1.0685(3) | 0.2884(2) | 0.5429(2) | 64(1) |
| C(35) | 0.9650(2) | 0.2407(2) | 0.4529(2) | 51(1) |
| C(36) | 0.5302(2) | 0.1030(2) | 0.3572(2) | 47(1) |
| C(37) | 0.4895(3) | 0.0021(2) | 0.3501(2) | 62(1) |
| C(38) | 0.3669(4) | −0.0366(3) | 0.3712(2) | 89(1) |
| C(39) | 0.2831(4) | 0.0224(4) | 0.3983(2) | 103(2) |
| C(40) | 0.3214(3) | 0.1229(3) | 0.4063(2) | 94(1) |
| C(41) | 0.4444(3) | 0.1630(2) | 0.3852(2) | 66(1) |
| C(42) | 0.6191(2) | 0.3565(2) | 0.3045(2) | 37(1) |
| N | 0.6192(2) | 0.4213(2) | 0.3594(2) | 59(1) |
| C(43) | 0.5519(5) | 0.4058(3) | 0.7031(3) | 104(1) |
| Cl(1) | 0.66408(10) | 0.45659(7) | 0.82496(8) | 100(1) |
| Cl(2) | 0.47170(15) | 0.28392(9) | 0.68161(12) | 153(1) |

$U_{eq}$ is defined as one-third of the trace of the orthogonalized $U_{ij}$ tensor.

Table 3
Atomic coordinates and equivalent isotropic displacement parameters ($Å^2 \times 10^3$) for $[RuCp(PPh_3)_2(CNH)]CF_3SO_3$ (2)

| | x | y | z | $U_{eq}$ |
|---|---|---|---|---|
| Ru | 0.33607(2) | 0.15598(2) | 0.10735(2) | 38(1) |
| C(1) | 0.4928(3) | 0.1089(3) | 0.1599(3) | 65(1) |
| C(2) | 0.4193(4) | 0.0857(4) | 0.2033(3) | 83(2) |
| C(3) | 0.3491(5) | 0.0388(3) | 0.1613(5) | 104(2) |
| C(4) | 0.3784(5) | 0.0318(3) | 0.0870(4) | 96(2) |
| C(5) | 0.4688(4) | 0.0767(3) | 0.0884(3) | 64(1) |
| P(1) | 0.28784(7) | 0.24775(6) | 0.19303(5) | 41(1) |
| C(6) | 0.1835(3) | 0.3186(2) | 0.1583(2) | 47(1) |
| C(7) | 0.0801(3) | 0.2961(3) | 0.1450(2) | 58(1) |
| C(8) | 0.0031(4) | 0.3483(3) | 0.1125(3) | 69(1) |
| C(9) | 0.0290(4) | 0.4240(3) | 0.0950(3) | 73(1) |
| C(10) | 0.1308(4) | 0.4473(3) | 0.1084(3) | 70(1) |
| C(11) | 0.2080(3) | 0.3950(2) | 0.1394(2) | 59(1) |
| C(12) | 0.3866(3) | 0.3115(2) | 0.2465(2) | 49(1) |
| C(13) | 0.3600(4) | 0.3710(2) | 0.2946(2) | 62(1) |
| C(14) | 0.4362(5) | 0.4151(3) | 0.3385(3) | 76(1) |
| C(15) | 0.5394(4) | 0.4005(3) | 0.3362(3) | 80(2) |
| C(16) | 0.5675(4) | 0.3428(3) | 0.2890(3) | 77(1) |
| C(17) | 0.4914(3) | 0.2992(3) | 0.2441(2) | 61(1) |
| C(18) | 0.2383(3) | 0.1940(2) | 0.2712(2) | 46(1) |
| C(19) | 0.1640(3) | 0.1354(2) | 0.2538(2) | 53(1) |
| C(20) | 0.1278(3) | 0.0933(3) | 0.3106(3) | 62(1) |
| C(21) | 0.1664(3) | 0.1072(3) | 0.3860(2) | 62(1) |
| C(22) | 0.2410(4) | 0.1630(3) | 0.4046(2) | 63(1) |
| C(23) | 0.2773(3) | 0.2065(2) | 0.3479(2) | 52(1) |
| P(2) | 0.37014(7) | 0.24175(6) | 0.01231(5) | 43(1) |
| C(24) | 0.2725(3) | 0.3058(2) | −0.0436(2) | 56(1) |
| C(25) | 0.1698(4) | 0.3056(3) | −0.0332(3) | 73(1) |
| C(26) | 0.0975(5) | 0.3530(4) | −0.0804(3) | 103(2) |
| C(27) | 0.1291(7) | 0.3979(4) | −0.1362(4) | 115(3) |
| C(28) | 0.2290(7) | 0.3971(3) | −0.1478(3) | 106(2) |
| C(29) | 0.3015(5) | 0.3511(3) | −0.1020(3) | 81(2) |
| C(30) | 0.4774(3) | 0.3099(2) | 0.0441(2) | 47(1) |
| C(31) | 0.4599(3) | 0.3899(2) | 0.0551(2) | 56(1) |
| C(32) | 0.5418(4) | 0.4387(3) | 0.0856(3) | 69(1) |
| C(33) | 0.6409(4) | 0.4092(3) | 0.1044(3) | 71(1) |
| C(34) | 0.6586(4) | 0.3303(3) | 0.0937(3) | 68(1) |
| C(35) | 0.5777(3) | 0.2812(2) | 0.0636(2) | 56(1) |
| C(36) | 0.4108(3) | 0.1883(2) | −0.0681(2) | 47(1) |
| C(37) | 0.3476(3) | 0.1268(3) | −0.0992(2) | 62(1) |
| C(38) | 0.3678(4) | 0.0876(3) | −0.1641(3) | 72(1) |
| C(39) | 0.4521(4) | 0.1086(3) | −0.1972(3) | 73(1) |
| C(40) | 0.5153(5) | 0.1676(3) | −0.1668(3) | 87(2) |
| C(41) | 0.4952(4) | 0.2075(3) | −0.1024(3) | 73(1) |
| C(42) | 0.1920(3) | 0.1405(2) | 0.0630(2) | 53(1) |
| N | 0.1086(3) | 0.1216(3) | 0.0397(2) | 80(1) |
| S | −0.17174(10) | 0.12546(9) | 0.04864(11) | 91(1) |
| O(1) | −0.0927(4) | 0.0706(3) | 0.0371(3) | 142(2) |
| O(2) | −0.2739(4) | 0.1124(5) | 0.0194(4) | 216(4) |
| O(3) | −0.1409(5) | 0.2033(3) | 0.0352(3) | 165(2) |
| C(43) | −0.1677(4) | 0.1250(4) | 0.1494(5) | 100(2) |
| F(1) | −0.2332(5) | 0.1711(3) | 0.1746(3) | 180(2) |
| F(2) | −0.0786(4) | 0.1380(5) | 0.1863(3) | 244(4) |
| F(3) | −0.1914(6) | 0.0587(3) | 0.1759(4) | 248(4) |
| Ag [a] | 0.0000 | 0.0000 | 0.0000 | 58(2) |

$U_{eq}$ is defined as one-third of the trace of the orthogonalized $U_{ij}$ tensor.

[a] A difference Fourier peak at this site was attributed to Ag with a refined site occupancy of 11.1(2)% corresponding to an Ag content of 0.055 mol per formula unit.

Table 4
Atomic coordinates and equivalent isotropic displacement parameters ($Å^2 \times 10^3$) for $[\{RuCp(PPh_3)_2CN\}_2H]CF_3SO_3 \cdot 1.5CH_2Cl_2$ (**3** · $1.5CH_2Cl_2$)

| | x | y | z | $U_{eq}$ |
|---|---|---|---|---|
| Ru(1) | 0.39391(3) | 0.65565(2) | 0.22788(2) | 31(1) |
| C(1) | 0.3768(4) | 0.8066(3) | 0.2064(3) | 45(1) |
| C(2) | 0.3015(4) | 0.7767(3) | 0.2669(3) | 51(1) |
| C(3) | 0.2365(4) | 0.7290(4) | 0.2507(3) | 55(1) |
| C(4) | 0.2729(4) | 0.7302(3) | 0.1781(3) | 52(1) |
| C(5) | 0.3581(4) | 0.7775(3) | 0.1514(3) | 46(1) |
| P(1) | 0.43262(9) | 0.59383(8) | 0.33313(6) | 34(1) |
| C(6) | 0.5041(4) | 0.4815(3) | 0.3445(2) | 42(1) |
| C(7) | 0.4549(5) | 0.4045(3) | 0.3671(3) | 58(1) |
| C(8) | 0.5096(6) | 0.3207(4) | 0.3771(3) | 78(2) |
| C(9) | 0.6123(6) | 0.3117(4) | 0.3645(3) | 78(2) |
| C(10) | 0.6624(5) | 0.3862(4) | 0.3405(3) | 68(2) |
| C(11) | 0.6099(4) | 0.4721(4) | 0.3294(3) | 52(1) |
| C(12) | 0.5002(3) | 0.6598(3) | 0.3657(2) | 39(1) |
| C(13) | 0.5515(4) | 0.6204(4) | 0.4163(3) | 54(1) |
| C(14) | 0.5985(5) | 0.6714(4) | 0.4414(3) | 68(2) |
| C(15) | 0.5962(5) | 0.7636(4) | 0.4169(3) | 73(2) |
| C(16) | 0.5456(5) | 0.8036(4) | 0.3678(3) | 66(2) |
| C(17) | 0.4995(4) | 0.7517(3) | 0.3420(3) | 49(1) |
| C(18) | 0.3154(3) | 0.5761(3) | 0.4050(2) | 38(1) |
| C(19) | 0.3140(4) | 0.5724(3) | 0.4739(2) | 50(1) |
| C(20) | 0.2265(5) | 0.5544(4) | 0.5272(3) | 62(2) |
| C(21) | 0.1408(5) | 0.5413(4) | 0.5133(3) | 65(2) |
| C(22) | 0.1406(4) | 0.5450(4) | 0.4462(3) | 69(2) |
| C(23) | 0.2289(4) | 0.5616(4) | 0.3924(3) | 55(1) |
| P(2) | 0.55221(9) | 0.63035(8) | 0.15298(6) | 34(1) |
| C(24) | 0.6409(4) | 0.5288(3) | 0.1657(2) | 39(1) |
| C(25) | 0.6069(4) | 0.4478(3) | 0.1711(3) | 50(1) |
| C(26) | 0.6726(5) | 0.3688(4) | 0.1708(3) | 69(2) |
| C(27) | 0.7724(5) | 0.3712(5) | 0.1663(4) | 79(2) |
| C(28) | 0.8080(5) | 0.4505(5) | 0.1631(3) | 74(2) |
| C(29) | 0.7429(4) | 0.5298(4) | 0.1616(3) | 54(1) |
| C(30) | 0.6239(3) | 0.7255(3) | 0.1395(2) | 40(1) |
| C(31) | 0.6661(4) | 0.7334(4) | 0.1905(3) | 50(1) |
| C(32) | 0.7119(5) | 0.8086(4) | 0.1850(3) | 66(2) |
| C(33) | 0.7150(5) | 0.8778(4) | 0.1288(3) | 70(2) |
| C(34) | 0.6732(4) | 0.8715(4) | 0.0772(3) | 59(1) |
| C(35) | 0.6284(4) | 0.7955(3) | 0.0822(3) | 47(1) |
| C(36) | 0.5519(3) | 0.6259(3) | 0.0644(2) | 38(1) |
| C(37) | 0.6441(4) | 0.6176(3) | 0.0139(2) | 47(1) |
| C(38) | 0.6484(4) | 0.6097(4) | −0.0520(3) | 55(1) |
| C(39) | 0.5607(5) | 0.6095(4) | −0.0692(3) | 61(2) |
| C(40) | 0.4684(4) | 0.6166(4) | −0.0204(3) | 56(1) |
| C(41) | 0.4643(4) | 0.6241(3) | 0.0467(2) | 44(1) |
| C(42) | 0.3582(3) | 0.5379(3) | 0.2279(2) | 37(1) |
| N(1) | 0.3292(3) | 0.4724(3) | 0.2273(2) | 53(1) |
| Ru(2) | 0.08565(3) | 0.18732(2) | 0.30125(2) | 37(1) |
| C(43) | −0.0678(4) | 0.1379(4) | 0.3438(3) | 59(1) |
| C(44) | −0.0753(4) | 0.2221(4) | 0.2969(3) | 65(2) |
| C(45) | −0.0500(4) | 0.2877(4) | 0.3235(4) | 71(2) |
| C(46) | −0.0262(4) | 0.2463(4) | 0.3870(3) | 64(2) |
| C(47) | −0.0380(4) | 0.1550(4) | 0.3986(3) | 59(2) |
| P(3) | 0.13267(9) | 0.14195(8) | 0.19574(6) | 38(1) |
| C(48) | 0.2644(4) | 0.1059(3) | 0.1519(2) | 40(1) |
| C(49) | 0.3342(4) | 0.1677(3) | 0.1381(3) | 48(1) |
| C(50) | 0.4330(4) | 0.1520(4) | 0.1001(3) | 55(1) |
| C(51) | 0.4657(4) | 0.0722(4) | 0.0762(3) | 61(2) |
| C(52) | 0.3987(4) | 0.0101(4) | 0.0895(3) | 59(2) |
| C(53) | 0.2987(4) | 0.0264(3) | 0.1270(2) | 50(1) |
| C(54) | 0.0588(4) | 0.0524(3) | 0.1989(3) | 48(1) |
| C(55) | 0.0822(4) | −0.0362(3) | 0.2316(3) | 52(1) |
| C(56) | 0.0193(5) | −0.1008(4) | 0.2424(3) | 70(2) |
| C(57) | −0.0687(6) | −0.0802(5) | 0.2220(5) | 99(3) |
| C(58) | −0.0941(6) | 0.0065(6) | 0.1908(5) | 102(3) |
| C(59) | −0.0300(5) | 0.0728(4) | 0.1787(4) | 74(2) |
| C(60) | 0.1060(4) | 0.2294(3) | 0.1228(3) | 48(1) |
| C(61) | 0.1208(4) | 0.2057(4) | 0.0589(3) | 64(2) |
| C(62) | 0.1060(5) | 0.2706(5) | 0.0019(3) | 79(2) |
| C(63) | 0.0778(5) | 0.3596(5) | 0.0086(3) | 76(2) |
| C(64) | 0.0643(4) | 0.3839(4) | 0.0712(3) | 73(2) |
| C(65) | 0.0778(4) | 0.3188(3) | 0.1288(3) | 52(1) |
| P(4) | 0.20513(10) | 0.10287(8) | 0.35538(6) | 40(1) |
| C(66) | 0.3411(4) | 0.0994(3) | 0.3096(2) | 46(1) |
| C(67) | 0.3975(5) | 0.1669(4) | 0.3040(3) | 71(2) |
| C(68) | 0.4994(5) | 0.1646(6) | 0.2675(4) | 93(2) |
| C(69) | 0.5457(5) | 0.0899(6) | 0.2377(4) | 84(2) |
| C(70) | 0.4905(4) | 0.0228(5) | 0.2411(3) | 70(2) |
| C(71) | 0.3889(4) | 0.0271(4) | 0.2760(3) | 52(1) |
| C(72) | 0.1949(4) | −0.0174(3) | 0.3912(2) | 45(1) |
| C(73) | 0.2682(4) | −0.0715(4) | 0.4217(3) | 59(1) |
| C(74) | 0.2594(5) | −0.1624(4) | 0.4487(3) | 65(2) |
| C(75) | 0.1797(5) | −0.2003(4) | 0.4460(3) | 66(2) |
| C(76) | 0.1061(5) | −0.1490(4) | 0.4168(3) | 61(2) |
| C(77) | 0.1133(4) | −0.0572(3) | 0.3899(3) | 49(1) |
| C(78) | 0.1955(4) | 0.1482(4) | 0.4333(3) | 51(1) |
| C(79) | 0.1768(4) | 0.0950(4) | 0.4994(3) | 61(2) |
| C(80) | 0.1626(5) | 0.1336(6) | 0.5572(3) | 84(2) |
| C(81) | 0.1666(5) | 0.2224(6) | 0.5504(4) | 88(2) |
| C(82) | 0.1842(5) | 0.2768(5) | 0.4852(4) | 87(2) |
| C(83) | 0.1982(5) | 0.2400(4) | 0.4265(3) | 71(2) |
| C(84) | 0.1792(4) | 0.2811(3) | 0.2626(2) | 42(1) |
| N(2) | 0.2296(4) | 0.3390(3) | 0.2425(2) | 56(1) |
| S(1) | 0.0764(3) | 0.3914(3) | 0.7118(2) | 160(1) |
| O(1) | 0.1395(11) | 0.4608(10) | 0.7000(5) | 330(9) |
| O(2) | 0.1167(14) | 0.3118(8) | 0.7088(7) | 354(10) |
| O(3) | −0.0051(12) | 0.4214(19) | 0.6714(5) | 500(17) |
| C(85) | 0.0029(5) | 0.3910(6) | 0.7932(3) | 147(4) |
| F(1) | 0.0602(7) | 0.3629(7) | 0.8336(5) | 290(6) |
| F(2) | −0.0616(8) | 0.3354(10) | 0.8055(5) | 501(15) |
| F(3) | −0.0435(10) | 0.4679(8) | 0.8032(5) | 436(12) |
| C(86) | 0.2314(9) | 0.8154(15) | 0.9876(12) | 496(35) |
| Cl(1) | 0.1801(12) | 0.7186(13) | 1.0015(10) | 1014(31) |
| Cl(2) | 0.1481(18) | 0.8983(11) | 1.0206(7) | 757(15) |
| Cl(3) | 0.4362(16) | 0.9645(7) | 0.5559(8) | 716(20) |

$U_{eq}$ is defined as one-third of the trace of the orthogonalized $U_{ij}$ tensor.
C(86), Cl(1), and Cl(2) define a $CH_2Cl_2$ molecule in general position, Cl(3) belongs to a second $CH_2Cl_2$ molecule which is disordered and arranged around a center of symmetry; its carbon atom was not located.

### 2.2. X-ray structure determinations

Crystal data and experimental details of the structure determinations of the three crystalline compounds **1** · $CH_2Cl_2$, **2**, and **3** · $1.5CH_2Cl_2$ are given in Table 1. The structures were solved with direct methods [6] and refined against $F^2$ using program SHELXL93 [7]. All non-hydrogen atoms were refined anisotropically. Hydrogen atoms were included in idealized positions and rode with the atoms to which they were bonded. Positional parameters are presented in Tables 2–4.

### 2.3. EH orbital calculations

The EH calculations were conducted by using the original program developed by Hoffmann and Lipscomb [8], and modified by Mealli and Proserpio [9]. The atomic parameters used in this study were taken from the CACAO program.

## 3. Results and discussion

### 3.1. Synthesis and spectroscopic data

Treatment of $RuCp(PPh_3)_2CN$ (**1**) with neat triflic acid (1.5 equivalents) gives $[RuCp(PPh_3)_2(CNH)]CF_3SO_3$ (**2**) in 89% isolated yield. Equimolar solutions of **1** and **2** yield the dimeric complex $[Ru_2Cp_2(PPh_3)_4(\mu\text{-}CN(H)NC)]CF_3SO_3$ (**3**) in practically quantitative yield. Complexes **2** and **3** are characterized by means of $^1H$ and $^{13}C\{^1H\}$ NMR and IR spectroscopy, and by elemental analysis.

The $^1H$ NMR spectrum of **2** reveals a singlet at 4.62 ppm (5H) assigned to the protons of the Cp ligand (cf. 4.39 ppm in complex **1**) and a multiplet in the range of 7.38–7.11 ppm (30H) assigned to the proton resonances of the $PPh_3$ ligands. The signal of the CNH proton could not be detected. The $^{13}C\{^1H\}$ NMR spectrum of **2** exhibits the expected multiplets for the carbon resonances of the $PPh_3$ ligands in the range of 138–126 ppm and a triplet at 87.6 ppm ($^2J(CP) = 1.7$ Hz) which is assigned to the carbon resonance of the Cp ligand. The parent cyano complex **1** exhibits the carbon resonance of Cp as a triplet at 85.3 ppm ($^2J(CP) = 1.9$ Hz). The resonance of the metal-bonded carbon of the CNH ligand has not been detected, even with long relaxation delays and extended accumulation times, whereas the respective resonance in **1** is observed as an apparent triplet at 142.0 ppm ($^2J(CP) = 19.9$ Hz).

The IR spectrum of **2** shows the $\nu$(CN) frequency decreased by 54 $cm^{-1}$ upon protonation as a weak absorption at 2016 $cm^{-1}$. A similar drop in the $\nu$(CN) frequency has been found for other CNH-complexes as in $MnCp(CO)_2(CNH)$ and $[Mn(\eta^6\text{-}C_6H_6)(CO)_2(CNH)]^+$ [10,11].

The $^1H$ and $^{13}C\{^1H\}$ NMR spectra of the new dimeric complex **3** are very similar to those of **1** and **2** (see Section 2). The resonance of the bridging hydrogen is not observed. In contrast to **2**, however, the $^{13}C\{^1H\}$ NMR resonance of the metal-bonded carbon of the $\mu$-hydrogen bis(isocyanide) ligand of **3** is found as an apparent triplet at 149.8 ppm ($^2J(CP) = 9.7$ Hz). The $\nu$(CN) frequency of complex **3** is observed as a strong absorption band at 2084 $cm^{-1}$, similar to that of complex **1** (2070 $cm^{-1}$). Thus the C–N bond order appears to be hardly affected by hydrogen coordination.

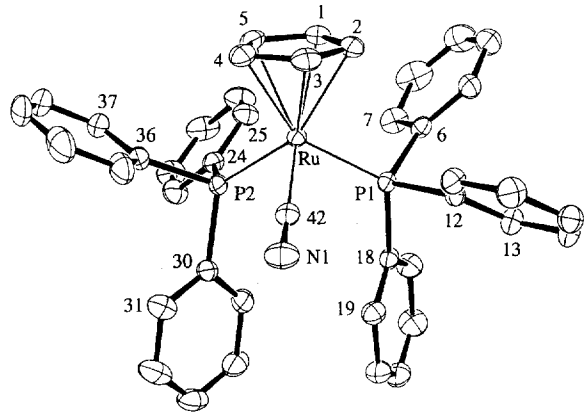


Fig. 1. ORTEP plot (30% ellipsoids) of $RuCp(PPh_3)_2CNCH_2Cl_2$ ($\mathbf{1}\cdot CH_2Cl)_2$) (solvent molecule omitted for clarity).

### 3.2. Solid-state structures

The molecular structures of $\mathbf{1}\cdot CH_2Cl_2$, **2**, and $\mathbf{3}\cdot 1.5CH_2Cl_2$ are shown in the Figs. 1–3. Selected bond lengths and angles for **1**, **2**, and **3** are compiled in Table 5. The complexes exhibit normal half-sandwich structures with a three-legged piano stool configuration. The lengths of both Ru–C (of $\eta^5$-bonded Cp) and Ru–P bonds are similar on average in the three compounds and are in accord with literature values. The Ru–C and C–N lengths of the cyano groups differ in the protonated and nonprotonated forms. Compared with $\mathbf{1}\cdot CH_2Cl_2$, the Ru–C (of CN) bond lengths in **2** and $\mathbf{3}\cdot 1.5CH_2Cl_2$ are systematically shorter by 0.05 to 0.10 Å, and those of C–N are longer by 0.04 Å. The CNH group in **2** forms quite a strong and distinctly bent hydrogen bond to O(1) of the triflate group, N ··· O(1) = 2.747(6) Å (Fig. 2). For comparison, in the crystalline dioxane solvate of $Cr(CO)_5CNH$ a CNH ··· O

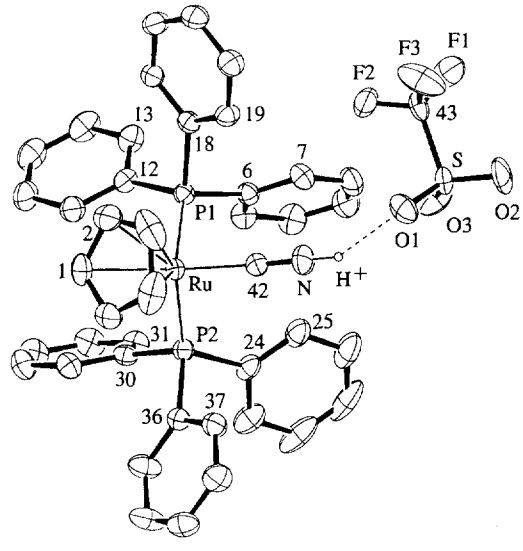


Fig. 2. ORTEP plot (30% ellipsoids) of $[RuCp(PPh_3)_2(CNH)]CF_3SO_3$ (**2**).

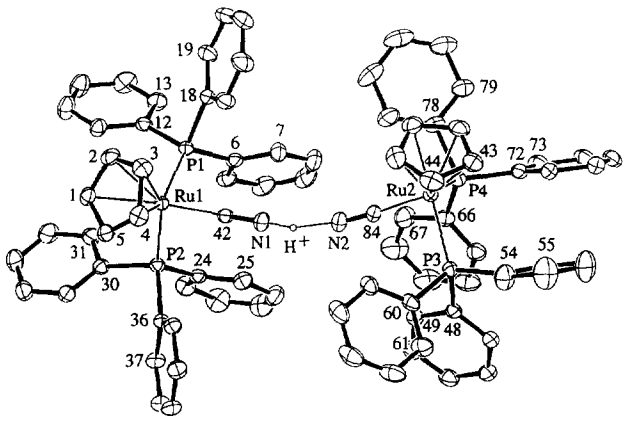


Fig. 3. ORTEP plot (30% ellipsoids) of $[Ru_2Cp_2(PPh_3)_4(\mu\text{-}CNHNC)]CF_3SO_3 \cdot 1.5CH_2Cl_2$ ($\mathbf{3} \cdot 1.5CH_2Cl_2$) ($CF_3SO_3^-$ and $CH_2Cl_2$ ommitted for clarity).

bond with 2.877(11) Å N · · · O distance is reported [12]. The complex $\mathbf{3} \cdot 1.5CH_2Cl_2$ contains two crystallographically independent $Ru(\eta^5\text{-}Cp)(PPh_3)_2(CN)$ fragments linked via a strong and supershort hydrogen bond N(1) · · · N(2) = 2.573(4) Å (with the triflate ion, not shown in Fig. 3, not engaged in hydrogen bonding). This is one of the shortest hydrogen bonds hitherto known, comparable with 2.569(7) Å in $[AsPh_4]^+[(CO)_5CrCN(H)NCCr(CO)_5]^-$, and 2.557(12) Å in $Fe(\eta^5\text{-}Cp)(Ph_2PCH_2CH_2PPh_2)CNHNCCr(CO)_5$ [12]. Similar to the latter case, the bridging hydrogen atom in $\mathbf{3} \cdot 1.5CH_2Cl_2$ is asymmetrically positioned between the two nitrogen atoms, being closer to N(1), indicating an asymmetric and somewhat bent N–H–N group CN∠CN angle of 156.6°. In the final structure refinement of $\mathbf{3} \cdot 1.5CH_2Cl_2$, this H atom was optimized as a part of an idealized linear C(42)–N(1)–H group.

Although the Cp ligands are clearly $\eta^5$ bonded, there are bond length alternations of both the endocyclic C–C and the Ru–C bonds in **1**, **2**, and **3**. Such an asymmetry of coordinated Cp is typical (some arbitrary examples are given in Ref. [13]) and has often been interpreted as a mere solid-state artefact resulting from the high librational motion of the Cp ligand. This rotational disorder (as indicated from the sizes, shapes, and orientations of the thermal ellipsoids of the carbon atoms) prevents observation of accurate data on molecular geometry and electron density. However, the possibility of involvement of distortion toward diene or allyl–ene structures coupled with a dynamic Jahn–Teller effect may not be neglected [14].

The C–N bond lengths of the coordinated cyanide ions ranging from 1.107 Å in **1** to 1.149 Å in **3** are all shorter than in free cyanide (1.172 Å) and in simple compounds (e.g. HCN, 1.153; MeCN, 1.159; acrylonitrile, 1.167 [15]; HNC, 1.1689 Å [16]). (These are gas-phase values, however, and may therefore not directly be compared with crystallographic data due to some librational shortenings of room temperature diffraction

Table 5
Selected bond lengths (Å) and angles (deg) for RuCp $(PPh_3)_2CN \cdot CH_2Cl_2$ ($\mathbf{1} \cdot CH_2Cl_2$), $[RuCp(PPh_3)_2CNH]CF_3SO_3$ (**2**), and $[\{RuCp(PPh_3)_2CN\}_2H]CF_3SO_3 \cdot 1.5CH_2Cl_2$ ($\mathbf{3} \cdot 1.5CH_2Cl_2$)

| | 1 | 2 | 3 | 3 [a] |
|---|---|---|---|---|
| Ru–C(1) | 2.236(2) | 2.248(4) | 2.237(6) | 2.239(5) |
| Ru–C(2) | 2.227(2) | 2.215(4) | 2.236(5) | 2.228(5) |
| Ru–C(3) | 2.231(2) | 2.203(5) | 2.246(5) | 2.222(5) |
| Ru–C(4) | 2.234(2) | 2.223(4) | 2.234(5) | 2.230(5) |
| Ru–C(5) | 2.229(2) | 2.254(4) | 2.230(4) | 2.231(5) |
| ⟨Ru–C⟩$_{av}$ | ⟨2.231⟩ | ⟨2.229⟩ | ⟨2.237⟩ | ⟨2.230⟩ |
| C(1)–C(2) | 1.427(3) | 1.375(7) | 1.405(7) | 1.427(8) |
| C(2)–C(3) | 1.407(3) | 1.344(8) | 1.409(7) | 1.402(8) |
| C(3)–C(4) | 1.402(3) | 1.431(9) | 1.425(7) | 1.390(9) |
| C(4)–C(5) | 1.416(3) | 1.396(7) | 1.396(7) | 1.420(9) |
| C(5)–C(1) | 1.413(3) | 1.370(6) | 1.414(7) | 1.395(8) |
| ⟨C–C⟩$_{av}$ | ⟨1.413⟩ | ⟨1.383⟩ | ⟨1.410⟩ | ⟨1.407⟩ |
| Ru–P(1) | 2.302(1) | 2.330(1) | 2.330(1) | 2.309(1) |
| Ru–P(2) | 2.318(1) | 2.321(1) | 2.306(1) | 2.313(1) |
| Ru–C(42) | 2.025(2) | 1.930(4) | 1.955(5) | 1.970(5) |
| C(42)–N | 1.107(4) | 1.143(5) | 1.149(6) | 1.149(6) |
| N · · · O(1) | | 2.747(6) | | |
| N(1) · · · N(2) | | | | 2.573(4) |
| Ru–C(42)–N(1) | 174.6(2) | 171.2(4) | 174.1(4) | 175.9(4) |
| P(1)–Ru–P(2) | 103.6(1) | 98.9(1) | 99.3(1) | 102.5(1) |
| P(1)–Ru–C(42) | 89.4(1) | 90.8(1) | 88.6(1) | 90.3(1) |
| P(2)–Ru–C(42) | 87.7(1) | 94.2(1) | 92.0(1) | 87.7(1) |
| CN∠NC | | | | 156.6(4) |

[a] Two independent Ru complexes in the asymmetric unit. Fourth column refers to Ru($n$ + 1), C($n$ + 42), P($n$ + 2), and N($n$ + 1) where $n$ is the index of the atoms given at the beginning of each line.

Table 6
MO energy levels (eV) of cyanide (bond length 1.143 Å) in various fragments

| Fragment | $\Psi_{CN}4$ n(N,C) | $\Psi_{CN}5$ $\pi$(C≡N) | $\Psi_{CN}6$ $\pi$(C≡N) | $\Psi_{CN}7$ n(N,C) | $\Psi_{CN}8$ $\sigma$(C–N) |
|---|---|---|---|---|---|
| $CN^-$ [a] | −11.972 | −14.766 | −14.766 | −18.418 | −30.003 |
| HCN | −14.192 | −14.766 | −14.766 | −20.307 | −30.073 |
| CNH | −13.735 | −14.766 | −14.768 | −20.069 | −30.348 |
| $Ru(CN)^+$ | −13.387 | −14.927 | −14.928 | −18.796 | −30.161 |
| $Ru(NC)^+$ | −13.131 | −14.997 | −14.998 | −18.742 | −30.181 |
| $Ru(CNH)^{2+}$ | −15.121 | −14.857 | −14.857 | −20.390 | −30.358 |
| Ru(CN)Cp | −13.349 | −14.923 | −14.932 | −18.771 | −30.167 |
| $Ru(CNH)Cp^+$ | −15.225 | −14.856 | −14.865 | −20.384 | −30.370 |
| $Ru(CN)PPh_3$ | −13.407 | −14.759 | −14.745 | −18.980 | −30.021 |
| | | −14.836 | −14.929 | | |
| $Ru(CN)(PPh_3)_2$ | −13.436 | −14.711 | −14.745 | −19.183 | −30.212 |

[a] See Table 5 footnote.

data. Thus, from comparisons with many other compounds, we would expect the real crystallographic value of the C–N bond length in **1** at about 1.145 Å.) Anyway, some remaining actual C–N bond length shortening of transition metal cyanide complexes [1] would signal an increase in ($\sigma$ and/or $\pi$) electron density between both atoms. This appears to be in contradiction to the nonlinearity found for the Ru–C–N bonds (the bond angle varies from 174.6° in **1** to 171.2° in **2**) which could be interpreted in terms of a change in hybridization towards $sp^2$ reducing the bond order through back donation. By the way, the structural changes brought by protonation, as noted above, tend to subside in **3**.

### 3.3. Molecular orbital calculations

The nature of the bonds in the three title complexes is examined by EH molecular orbital calculations. In particular we will explore the role of both Ru–C–N and CN–H–NC bending and the asymmetry of coordinated Cp. Along these lines we would like to get hints as to how to discern between packing effects and electronic effects in the solid state structures under scrutiny. In addition, we are interested in knowing the reason for the short CN(H) · · · NC bond. Notice that many properties of transition metal complexes with both CN and Cp ligands have successfully been studied using EH calculations [17–19].

We started with analyzing the free cyanide ion and reproduced the results derived from more exact 'ab initio' and other calculation methods [20–22]. Accordingly (first line in Table 6), the lowest orbital in the EH scheme ($\Psi_{CN}8 \equiv \sigma$) derives from s and sp orbital overlap between N2s and C2s, $2p_z$. The two other $\sigma$ MOs ($\Psi_{CN}7 \equiv \sigma^*$, $\Psi_{CN}4 \equiv \sigma$) result from antibonding ($\sigma^*$ N2s and C2s, $2p_z$), and bonding (p–p) MOs mixing provides the two free axial electron pairs on each C and N, owing to which the cyanide ion is a terminal two-electron donor ligand or an axial four-electron donor bridging ligand [17]. The other p electrons are participating in the two $\pi$ MOs ($\Psi_{CN}5$ and $\Psi_{CN}6$).

As is further seen in Table 6, when $CN^-$ coordinates to the electrophiles $H^+$, $Ru^{2+}$, the energies of the $\Psi_{CN}7$ and $\Psi_{CN}4$ MOs are substantially lowered, whereas the $\pi$ orbitals are only marginally affected. This means, in contrast to the common view, that C–N bond shortening attending complexation is not due to multiple bond strengthening, but rather $\sigma$ bond strengthening owing

Table 7
d–d splitting (eV) in ruthenium in various fragments

| Fragment | $\Psi_{Ru}1$ | $\Psi_{Ru}2$ | $\Psi_{Ru}3$ | $\Psi_{Ru}4$ | $\Psi_{Ru}5$ |
|---|---|---|---|---|---|
| $Ru^{+2}$ | −12.200 | −12.200 | −12.200 | −12.200 | −12.200 |
| $RuCp^+$ | −10.033 | −10.053 | −11.761 | −12.188 | −12.194 |
| $Ru(PPh_3)_2^{2+}$ | −10.203 | −11.676 | −11.850 | −11.946 | −11.977 |
| $Ru(CN)^+$ | −11.114 | −12.200 | −12.200 | −12.265 | −12.267 |
| $Ru(PPh_3)_2(CN)^+$ | −9.482 | −10.269 | −11.732 | −11.919 | −12.036 |
| $Ru(PPh_3)_2Cp^+$ | −6.757 | −9.834 | −11.278 | −11.616 | −11.853 |
| $Ru(CNH)^{2+}$ | −11.228 | −12.200 | −12.200 | −12.296 | −12.301 |
| Ru(CN)Cp | −9.147 | −10.200 | −11.810 | −11.883 | −12.233 |
| $Ru(CNH)Cp^+$ | −9.063 | −10.264 | −11.790 | −11.910 | −12.282 |
| Ru in **1** | −6.429 | −6.664 | −11.512 | −11.158 | −11.721 |
| Ru in **2** | −6.436 | −6.688 | −11.204 | −11.496 | −11.756 |

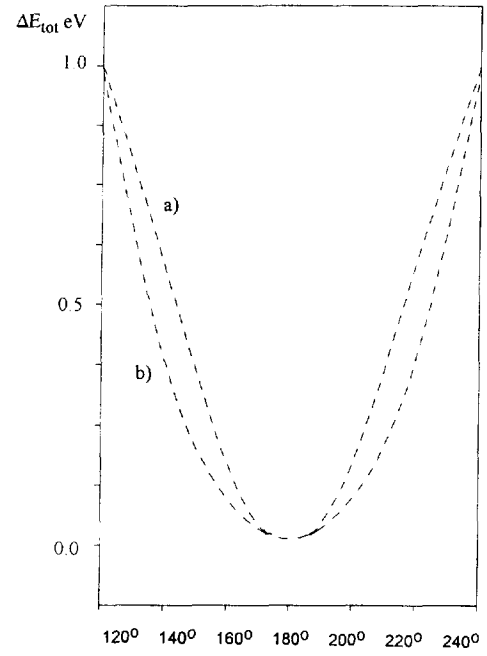


Fig. 4. Total energy of the RuCNHNCRu fragment as a function of the angle of the bond of (a) R–C–N and (b) N–H–N.

to the decrease in the antibonding character of $\sigma^*$. This is in line with other MO studies pointing to the leading role of $\sigma$ bonding in the metal–cyanide interactions [21–23]. Another important result is the correlated lowering of both MOs, $\Psi_{CN}7$ and $\Psi_{CN}4$, upon coordination implying that coordination of cyanide concomitantly increases the Lewis basicity of the free cyanide site favoring bridge formation. This is ultimately the reason for the occurrence of the 'supershort' CN(H) · · · NC bonds in the hydrogen bridged binuclear complex **3**. In fact, protonation of the Ru–CN fragment to give Ru–CNH additionally stabilizes these two MOs (Table 6) pointing to their mutual connection. Compared with this, $\pi$ backbonding is unimportant, though slightly increasing with protonation; this is seen by the somewhat lowered energies of $\Psi_{CN}5$ and $\Psi_{CN}6$, and likewise by the changes in the Ru d-levels $\Psi_{Ru}4$, $\Psi_{Ru}5$ (Table 7). In this way the $\sigma$ HOMO of $CN^-$ ($\Psi_{CN}4$) comes to lie below the $\pi$-MOs, with the latter activated as $\pi$ HOMO. Such $\sigma-\pi$ MO inversion of the cyanide ion is also encountered in certain hexacyano metal complexes [21]. Although small, the backbonding effect in the present case should nevertheless be responsible for the increase and decrease, respectively, of the C–N and Ru–CN bond lengths in going from **1** to **2** (Table 5). Another remark concerns the Ru–CN and CN–H–NC bendings. To elucidate their origin we calculated the total energies of the fragment RuCNHNCRu as a function of the bond angles Ru–C–N and RuCN–H–NCRu between 120 and 240°. The results are displayed in Fig. 4. A flat minimum occurs at $180 \pm 15°$ for each case followed by a steep increase at both sides with no additional minimum at 120°. This is evidence in favor of the participation of only s and/or sp AOs of the cyanide moiety, without notable $sp^2$ contribution. It is thus implied that bridge formation is not accompanied by rehybridization, rendering the deviations from linearity of the bonds under consideration in the solid state as a packing forces effect.

Next we consider the influence of $PPh_3$ on the Ru–CN interactions, i.e. when going from $RuCN^+$ to $Ru(CN)(PPh_3)^+$ or $Ru(CN)(PPh_3)_2^+$ in Table 6. Notice that $PPh_3$ is a stronger $\sigma$ donor than cyanide, as judged from the Ru d–d splittings in Table 7. Notwithstanding, the presence of $PPh_3$ stabilizes the Ru–CN bond further, especially by lowering the energy of $\Psi_{CN}7$ (and to a lesser extent that of $\Psi_{CN}4$) due to additional overlap between these two $\sigma$ orbitals with the p orbitals of phosphorus. Also noteworthy is the concomitant splitting of the $\pi$ MOs (Table 6) occurring without participation of the Ru AOs, as shown by a Mulliken analysis. The reason for this splitting may be sought in terms of

Table 8
MO energy levels (eV) of cyclopentadienyl in various fragments

| Fragment | $\Psi_{Cp}13$ $\pi$ | $\Psi_{Cp}14$ $\pi$ | $\Psi_{Cp}17$ $\sigma$ | $\Psi_{Cp}18$ $\sigma$ | $\Psi_{Cp}19$ $\pi$ |
|---|---|---|---|---|---|
| $Cp_{sym}$ | −11.991 | −11.991 | −14.219 | −14.219 | −14.555 |
| Cp as in **1** | −11.961 | −12.022 | −14.098 | −14.133 | −14.500 |
| $Ru(Cp_{sym})^+$ | −13.077 | −13.077 | −14.405 | −14.405 | −14.708 |
| $Ru(Cp_{sym})_2$ | −12.400 | −13.214 | −14.260 | −14.652 | −14.555 |
| | −12.400 | −13.214 | −14.260 | −14.652 | −14.839 |
| $RuCp^+$ | −13.043 | −13.073 | −14.389 | −14.417 | −14.641 |
| Ru(CN)Cp | −12.842 | −13.059 | −14.380 | −14.404 | −14.624 |
| $RuCp(CNH)^+$ | −12.908 | −13.123 | −14.184 | −14.349 | −14.618 |
| $RuCp(PPh_3)_2^+$ | −12.894 | −12.922 | −14.308 | −14.364 | −14.510 |
| | −13.019 | −13.132 | | | −14.555 |
| **1** | −12.730 | −12.803 | −14.307 | −14.355 | −14.506 |
| | −12.794 | −12.897 | | | −14.550 |
| **2** | −12.846 | −13.106 | −14.178 | −14.361 | −14.545 |
| | −12.902 | −13.193 | | | −14.574 |

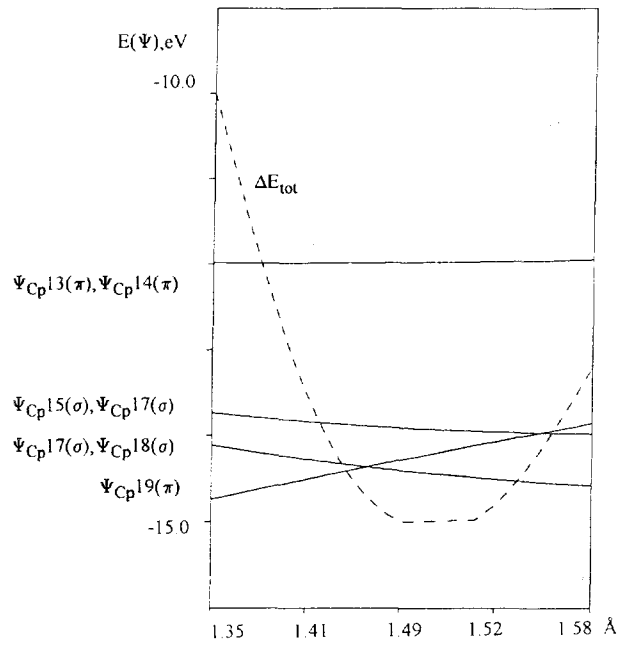


Fig. 5. Various orbital energies of free Cp as a function of the C–C bond length.

$\pi$(CN)–$\pi$(phenyl) conjugation. Similar $\pi$–$\pi$ interactions between different co-ligands may be the origin of phenomena known as the 'aromatic ring current effect' [24] and 'remote shielding' [25]. Upon protonation of the coordinated cyanide (going from **1** to **2**), this conjugation and the corresponding $\pi$ MO splitting is reduced. Consequently, the Ru–P bond is longer in **2** than in **1** (Table 5).

Compared with $PPh_3$, the presence of Cp in trans position has no effect on the cyanide fragment, except that the two $\pi$ MOs of cyanide become slightly different in energy (see Ru(CN)(Cp) in Table 6). This would indicate some nonequivalence in the Cp and CN orbitals interaction forwarded through the Ru center. Regarding the Cp orbitals involved in the Ru–Cp interactions, the EH analysis reveals the leading role of the two high-lying (occupied) $\pi$ MOs ($e_{1g} \equiv \Psi_{Cp}13$ and $\Psi_{Cp}14$), and the subordinate importance of the symmetrical (occupied) $\pi$ MO ($a_{1g} \equiv \Psi_{Cp}19$). Notice, however, that in between $e_{1g}$ and $a_{1g}$ are placed four $\sigma$ MOs. Whereas $\Psi_{Cp}15$ and $\Psi_{Cp}16$ do not participate in Ru–C bonding, $\Psi_{Cp}17$ and $\Psi_{Cp}18$, given in Table 8, render appreciable $\sigma$–$\sigma$ Ru–Cp overlap. These results are in accord with other MO calculations [26], as well as with photoelectron spectra [27].

After all, it would appear that the Cp ligand is well-suited to demonstrate the intimate relationships between electronic structure and geometry as follows. Even small changes in the C–C bond lengths within the range 1.3 to 1.6 Å affect inversion in levels of the $\pi$ MO ($\Psi_{Cp}19$) and $\sigma$-MOs ($\Psi_{Cp}17$ and $\Psi_{Cp}18$) both in free and coordinated Cp (Fig. 5) for maximum total energy to be obtained. Compared with this, changes in the C–H bond lengths (from 0.9 to 1.1 Å) or a little strain of the Cp ring have little effect on the relative MO energies. Therefore, we suggest the experimental C–C bond lengths and their variations within the Cp ring be used as a clue to the relative contributions of $\pi$ and $\sigma$ bonding in metal–Cp interactions. A pertinent example may be the dynamics of beryllocene [28]. The ease of inversion of the MO levels is revealed by the small amount of energy (5–8 kJ $mol^{-1}$) necessary for conversions between $\eta^5$, $\eta^3$ and $\eta^1$ structures to occur [28,29]. By the same token, associative reactions of Cp complexes are believed to proceed by an $\eta^5 \rightarrow \eta^3 \rightarrow \eta^5$ or $\eta^5 \rightarrow \eta^3 \rightarrow \eta^1$ ring-slippage mechanism [30]. Along these lines, it is tempting to rationalize the asymmetry of the coordinated Cp ring in terms of such a $\sigma \rightleftharpoons \pi$ MO inversion. It can be gleaned from Table 8 that bonding between $Ru^{2+}$ and Cp is primarily due to the $e_{1g}$ MOs ($\Psi_{Cp}13$ and $\Psi_{Cp}14$) and to a lesser extent to the C–C $\sigma$ orbitals of Cp ($\Psi_{Cp}17$ and $\Psi_{Cp}18$). However, the variations in these latter two MOs can make the Cp ring become asymmetric, establishing the tendency towards $\eta^5 \rightarrow \eta^3$ inversion.

Let us now briefly outline the changes in the Ru–Cp interactions as induced by the co-ligands (Table 8), complementing the discussion of Table 6. Cyanide is seen to destabilize the Ru–Cp $\pi$ bonds, with $\Psi_{Cp}13$ affected much more than $\Psi_{Cp}14$, thus giving rise to a splitting of these two orbitals. Some splitting is also discernible between $\Psi_{CN}5$ and $\Psi_{CN}6$ in Ru(CN)(Cp) in Table 6. These comparisons underscore the emerging

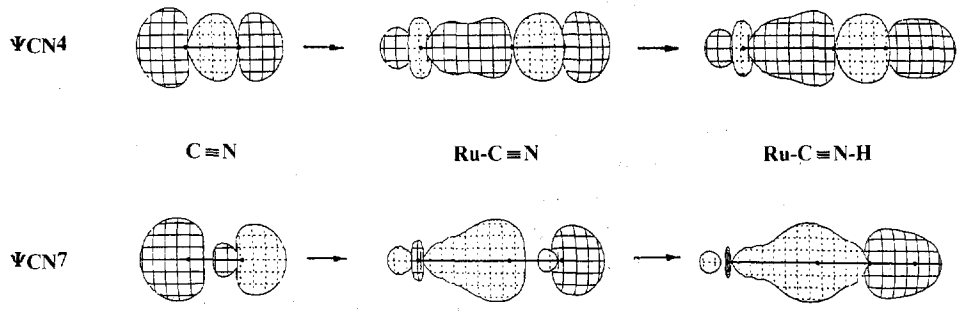


Fig. 6. Selected valence orbitals for the RuCNH fragment.

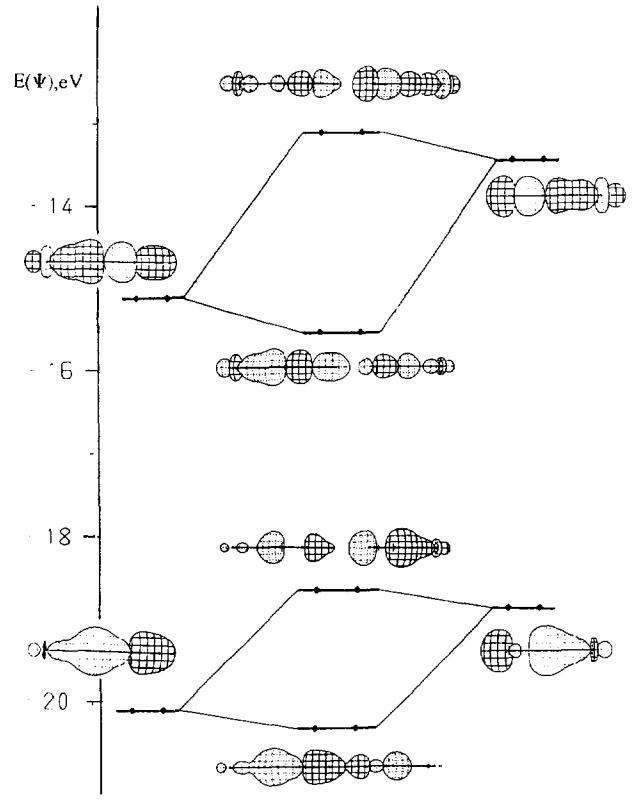


Fig. 7. Qualitative molecular orbital diagram for the RuCNHNCRu fragment including selected valence orbitals.

notion that, in the main, only one orbital each of Cp and CN interact with one another through the Ru center, thus provoking Cp distortion. The energy gain of $\Psi_{CN}6$ corresponds to the energy loss of $\Psi_{Cp}13$ because of electron density shift from CN to the Cp fragment. For $PPh_3$ as the co-ligand, the $\pi-\pi$ conjugation through the d orbitals of Ru seen by the splitting of the $e_{1g}$ and $a_{1g}$ MOs of Cp has been noted above.

Summing up, the relative orbital energies of cyanide remain essentially unchanged in the sequence

$$CN \rightarrow RuCN \rightarrow RuCNH \rightarrow RuCNH \cdots NCRu$$

Coordination of cyanide to the $d_{z^2}$ AO of $Ru^{2+}$ results in a stabilization of the $\sigma$ MOs ($\Psi_{CN}4$ and $\Psi_{CN}7$) of CN. The MOs formed in Ru–CN are mainly those of CN, with the C–N $\sigma$ bond further strengthened due to the decrease in the antibonding character of $\Psi_{CN}7$ transforming into a free electron pair of RuCN favoring the binding of another electrophile (in our case $H^+$), see Fig. 6. This protonated species represents a complexed isoprussic acid and can combine with another nucleophile [1], such as the Ru–CN fragment, by overlap of the two corresponding $\Psi_{CN}7$ MOs with additional gain in energy (Fig. 7). For the co-ligands, Cp has practically no effect, and $PPh_3$ has only a small effect, on the stability of the CN(H) · · · CN fragment bonds.

## 4. Conclusions

The peculiar features of the present crystal structures have successfully been examined using EH molecular orbital calculations. Accordingly, the bendings of the Ru–C–N and N(H) · · · N bonds in the solid state are to be interpreted simply as packing effects, re-emphasizing the weakness of the backbonding capacity of cyanide. In contrast, the asymmetry of coordinated Cp may include electronic effects originating from the noncylindrical bonding interactions with the RuCN fragment. The distorted endocyclic bond-length pattern is suggested to be indicative of the relative importance of $\sigma$ and $\pi$ bonding in the metal–cyclopentadienyl interactions.

## 5. Supplementary material

Listings of anisotropic temperature factors, hydrogen atom parameters, complete bond distances and angles of complexes **1–3** can be obtained from the authors on request.

## Acknowledgements

Gratitude is expressed to the "Fonds zur Förderung der wissenschaftlichen Forschung" for support (Project No. 9825-CHE).

## References

[1] W.P. Fehlhammer and M. Fritz, *Chem. Rev., 93* (1993) 1243.
[2] M.I. Bruce and R.C. Wallis, *Aust. J. Chem., 34* (1981) 209.
[3] G.J. Baird and S.G. Davies, *J. Organomet. Chem., 262* (1984) 215.
[4] B.F. King and F. Weinhold, *J. Chem. Phys., 103* (1995) 333.
[5] D.D. Perrin and W.L.F. Armarego, *Purification of Laboratory Chemicals*, Pergamon, 3rd edn., 1988.
[6] S.R. Hall, H.D. Flack and J.M. Stewart, XTAL3.2 *Integrated system of computer programs for crystal structure determination*, Universities of Wetern Australia, Geneva and Maryland, 1992.
[7] G.M. Sheldrick, SHELXL93 *Program for crystal structure refinement*, University of Göttingen, 1993.
[8] (a) R. Hoffmann and W.N. Lipscomb, *J. Chem. Phys., 36* (1962) 2179. (b) R. Hoffmann and W.N. Lipscomb, *J. Chem. Phys., 36* (1962) 3489. (c) R. Hoffmann, *J. Chem. Phys., 39* (1963) 1397.
[9] C. Mealli and D.M. Proserpio, *J. Chem. Educ., 67* (1990) 399.
[10] P.J.C. Walker and R.J. Mawby, *J. Chem. Soc. A*, (1971) 3006.
[11] E.O. Fischer and R.J.J. Schneider, *J. Organomet. Chem., 12* (1968) 27.
[12] E. Bär, J. Fuchs, D. Rieger, F. Aguilar-Parilla, H.-H. Limbach and W.P. Fehlhammer, *Angew. Chem., 103* (1991) 88.
[13] (a) L.S. Liebeskind and A. Bombrun, *J. Am. Chem. Soc., 113* (1991) 8736. (b) K. Kirchner, K. Mereiter, A. Umfahrer and R.

Schmid, *Organometallics, 13* (1994) 1886. (c) K. Mauthner, K. Mereiter, R. Schmid and K. Kirchner, *Inorg. Chim. Acta, 236* (1995) 95. (d) K. Kirchner, K. Mereiter, R. Schmid and H. Taube *Inorg. Chem., 32* (1993) 5553. (e) K. Kirchner, K. Mereiter, K. Mauthner and R. Schmid, *Inorg. Chim. Acta, 217* (1994) 203. (f) M.O. Albers, D.C. Liles, D.J. Robinson, A. Shaver and E. Singleton, *Organometallics, 6* (1987) 2347. (g) R. Gleiter, I. Hyla-Kryspin, M. Ziegler, G. Sergeson, J.C. Green, L. Stahl and R.D. Ernst, *Organometallics, 8* (1989) 298. (h) W.E. Buhro, M.C. Etter, S. Georgiou, J.A. Gladysz and F.B. McCormick, *Organometallics, 6* (1987) 1150. (i) J.M. Wisner, T.J. Bartczak and J.A. Ibers, *Inorg. Chim. Acta, 100* (1985) 115.

[14] (a) S. Noh, R.A. Heintz, B.S. Haggerty, A.L. Rheingold and K.H. Theopold, *J. Am. Chem. Soc., 114* (1992) 1892. (b) J.H. Ammeter, N. Oswald and R. Bucher, *Helv. Chim. Acta, 58* (1975) 671. (c) H. Eicher and H. Kohler, *Chem. Phys., 128* (1988) 297.

[15] D.R. Lide (ed.), *CRC Handbook of Chemistry and Physics*, CRC Press, 1995, pp. 9.19-9.24.

[16] T.J. Lee. *J. Am. Chem. Soc., 111* (1989) 7362.

[17] S.R. Nogueira, N.V. Vugman and D. Guenzburger, *Chem. Phys., 164* (1992) 229.

[18] N.T. Anh, M. Elian and R. Hoffmann, *J. Am. Chem. Soc., 100* (1978) 110.

[19] H. Shen, R.A. Senter, S.G. Bott and M.G. Richmond, *Inorg. Chim. Acta, 238* (1995) 57.

[20] M. Sano, Y. Hatano, H. Kashiwadi and H. Yamatera, *Bull. Chem. Soc. Jpn., 54* (1981) 1523.

[21] M. Sano, H. Adachi and H. Yamatera, *Bull. Chem. Soc. Jpn., 54* (1981) 2898.

[22] J.J. Alexander and H. Gray, *Coord. Chem. Rev., 2* (1967) 29.

[23] S.R. Nogueira and D. Guenzburger, *Int. J. Quant. Chem., 54* (1995) 381.

[24] S. Tachiyashiki and H. Yamatera, *J. Chem. Soc. Dalton Trans.*, (1990) 13.

[25] M. Maruyama, H. Matsuzawa and Y. Kaizu, *Inorg. Chim. Acta, 237* (1995) 159.

[26] (a) M.F. Rettig and R.S. Drago, *J. Am. Chem. Soc., 91* (1969) 3432. (b) J.H. Schachtschneider, R. Prins and R. Ros, *Inorg. Chim. Acta, 1* (1967) 462. (c) A.T. Armstrong, D.G. Carroll and S.P. McGlynn, *J. Chem. Phys., 47* (1967) 1104. (d) M. Coutiere, J. Demuynck and A. Veillard, *Theor. Chim. Acta, 27* (1972) 181.

[27] (a) S. Di Bella, A. Gulino, G. Lanza and I.L. Fragala, *J. Phys. Chem., 97* (1993) 11673. (b) D.L. Lichtenberger and R.F. Fenske, *J. Am. Chem. Soc., 98* (1976) 50. (c) J.W. Rabalais, L.O. Werme, T. Bergmark, L. Karlson, M. Hussain and K. Siegban, *J. Chem. Phys., 57* (1972) 1185.

[28] P. Margl and K. Schwarz, *J. Chem. Phys., 103* (1995) 683.

[29] N.T. Anh, M. Elian and R. Hoffmann, *J. Am. Chem. Soc., 100* (1978) 110.

[30] J.K. Shen, S. Zhang, F. Basolo, S.E. Johnson and M.F. Hawthorne, *Inorg. Chim. Acta, 235* (1995) 89.